Effects of mechanical activation on the formation of PbTiO 3 from amorphous Pb–Ti–O precursor

T. Yu, Z. X. Shen, J. M. Xue, and J. Wang

Citation: Journal of Applied Physics **93**, 3470 (2003); doi: 10.1063/1.1554471
View online: http://dx.doi.org/10.1063/1.1554471
View Table of Contents: http://scitation.aip.org/content/aip/journal/jap/93/6?ver=pdfcov
Published by the AIP Publishing

Effects of mechanical activation on the formation of $PbTiO_3$ from amorphous Pb–Ti–O precursor

T. Yu[a] and Z. X. Shen
Department of Physics, National University of Singapore, 2 Science Drive 3, Singapore 117542, Singapore

J. M. Xue and J. Wang
Department of Materials Science, National University of Singapore, 2 Science Drive 3, Singapore 117542, Singapore

(Received 19 September 2002; accepted 19 December 2002)

We investigate the effects of mechanical activation in triggering $PbTiO_3$ (PT) formation from an amorphous Pb–Ti–O precursor synthesized by coprecipitation. In this work, the amorphous precursor and the samples derived from it by mechanical activation were investigated using Raman spectroscopy, x-ray diffraction, and high-resolution transmission electron microscopy. Our results show that the crystallization of tetragonal PT phase can be considered as a nucleation and growth process described by the Avrami model. In the initial stage of mechanical activation, the main effect is size reduction of the constituent starting materials. For a longer period of milling, perovskite PT crystallites are formed by mechanical activation alone. These crystallites act as seeds, reducing the activation energy from 249 ± 6 kJ/mol for the precursor to 97 ± 7 kJ/mol for the 30-h-milled sample and enhances the crystallization kinetics, during postcalcination. Consequently, the PT phase formation temperature is dramatically lowered. In addition, our results demonstrate that the particle size affects the structure of the PT phase, where the PT shows the pseudocubic to tetragonal transition with increasing particle size. © *2003 American Institute of Physics.*
[DOI: 10.1063/1.1554471]

I. INTRODUCTION

Lead titanate, $PbTiO_3$ (PT) is a well-known ferroelectric and piezoelectric material.[1] It has many important technological applications in electronics and microelectronics, because of its high Curie temperature, high pyroelectric coefficient and high spontaneous polarization.[2,3] Several methods have been employed to prepare $PbTiO_3$ powders in the literature, including chemical coprecipitation,[4] sol-gel,[5] and hydrothermal reaction.[6] Recently, mechanical activation, which was invented with an initial attempt as a method to develop dispersion-strengthened high temperature alloys, has been successfully used to produce nanometer-sized $PbTiO_3$ powders.[7] The most important advantage of the mechanical activation is that it can be used to synthesize designed compounds at room temperature with a particle size in the nanometer scale. This characteristic is especially important to lead-containing materials, because lead oxide is very volatile at elevated temperature and is toxic. In this article, we report the formation of nanocrystalline PT phase by mechanical activation from an amorphous Pb–Ti hydroxide precursor synthesized by the coprecipitation method. The mechanical activation effects on the PT phase crystallization and the size effect on the PT nanoparticles were also studied by annealing the precursor sample and the samples derived from the precursor by mechanical activation.

[a]Electronic mail: scip9600@nus.edu.sg

II. EXPERIMENT

The Pb–Ti hydroxide amorphous precursor was synthesized using the coprecipitation method, by slowly adding a mixed nitrate solution of Pb^{2+} [from $Pb(NO_3)_2$, >99%, Merck, Germany], and Ti^{4+} (from TiCl4, >99%, Hayashi Pure Chemical Industries Ltd., Japan) into an ammonia solution of *p*H 9. The resulting coprecipitates were then aged for 1 h in the supernatant liquid, followed by filtration and drying at 90 °C for 2 h in an oven. The dried precursor powder was thermally treated at 300 °C for 2 h to dehydrate the precursor and at the same time preserve the Pb–Ti hydroxide precursor. Five grams of the precursor powder was loaded into a cylindrical vial 40 mm in diameter and 40 mm in length together with a milling ball 12.7 mm in diameter. Mechanical activation was carried out in a SPEX mill (8000M) operating at 900 rpm for 10, 20, and 30 h, respectively.[8] Calcination was preformed in air ambient. The samples thus obtained were characterized using an x-ray diffractometer (X'Pert, Philips), Raman spectroscopy (ISA T64000 triple grating system), as well as high-resolution transmission electron microscope, (HRTEM, Philips CM300FEG).

III. RESULTS AND DISCUSSION

A. Mechanical activation process

Figure 1 shows the XRD patterns of the as-synthesized precursor and the samples after mechanical activation for 10, 20, and 30 h. Only one broad hump ranging from a 2θ angle of 25°–35° was observed in the as-synthesized precursor,

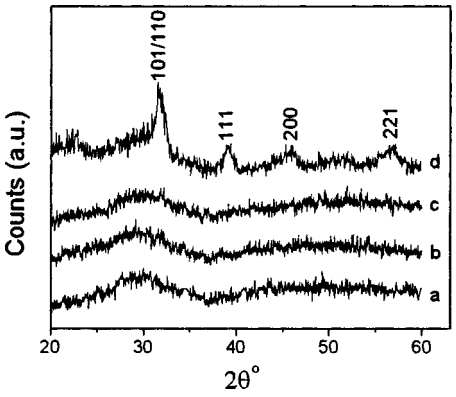

FIG. 1. XRD patterns of (a) precursor, (b) precursor mechanically activated for 10 h, (c) for 20 h, and (d) for 30 h.

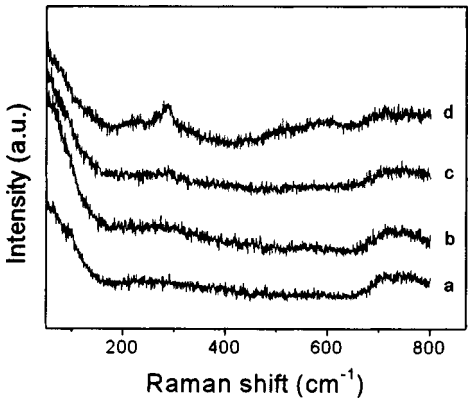

FIG. 3. Raman spectra of (a) precursor, (b) precursor mechanically activated for 10 h, (c) for 20 h, and (d) for 30 h.

indicating its highly amorphous nature. There was no significant difference between the XRD patterns of the precursor and the 10-h-milled sample, implying that little crystalline phase was triggered by mechanical activation for 10 h. Similarly, little change was observed in the XRD trace for the 20-h-milled sample, although the hump over the 2θ range of 25°–35° was slightly sharpened by the continued mechanical activation. Upon mechanical activation for 30 h, four peaks at 2θ angles of 32.1°, 39.3°, 46.1°, and 57.5° were well established, corresponding to the (101/110), (111), (200), and (211) planes of the crystalline $PbTiO_3$ perovskite structure.[9] The appearance of these diffraction peaks demonstrates that the perovskite nanocrystallites of $PbTiO_3$ can be triggered to form in the highly amorphous Pb–Ti–O precursor by mechanical activation alone at room temperature. This is in agreement with what has been observed in several other Pb-based ferroelectric compositions, where nucleation and subsequent growth of nanocrystallites can take place in the highly activated matrices.[10–12]

Figure 2 shows a TEM micrograph of the 30-h-milled sample. Nanocrystallites can be clearly found in the amorphous matrix. Identification of d spacing ($d=0.299$ nm) suggests the spherical crystallite shown in Fig. 2 corresponds to the (111) plane ($d=0.297$ nm) of $PbTiO_3$ phase.[13] In fact, our previous TEM results,[14] show that crystallites already exist in the 20-h-milled samples, although they were not shown by the phase analysis using XRD. As XRD is a bulk technique, the volume fraction of the crystallites in the 20-h-milled sample is too low to be detected.

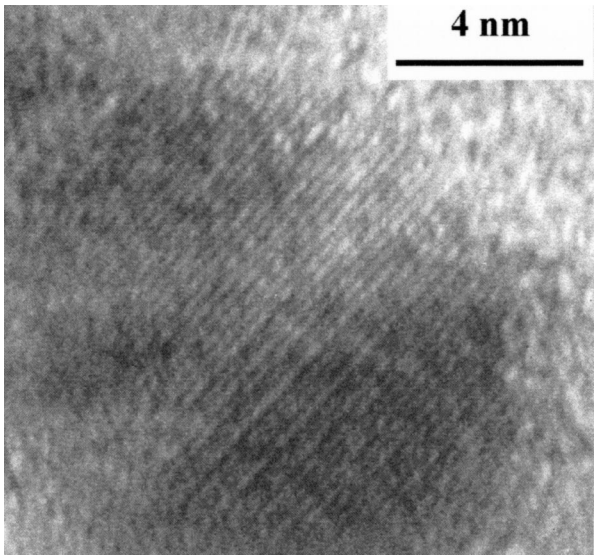

FIG. 2. TEM micrograph showing a $PbTiO_3$ nanocrystal in the 30-h-milled sample.

To further identify the nanocrystallites triggered by mechanical activation in the amorphous matrix, Raman spectroscopy was employed to study the mechanically activated samples, shown in Fig. 3. Similar to the XRD results, no sharp Raman peaks representing crystalline phases were observed in the samples up to 20 h of milling, although there seems to be a weak peak centered at ~ 300 cm^{-1} for the 20-h-milled sample, suggesting the existence of PT crystallites. In the 30-h-milled sample, one relatively sharp Raman peak and two broad Raman peaks centered at 300, 500, and 600 cm^{-1}, respectively, belonging to the crystalline PT phase,[15] were clearly observable. This agrees with the results derived from XRD and TEM that nucleation of $PbTiO_3$ crystal occur with increasing mechanical activation duration.

On the basis of the above results, the mechanical activation process of the amorphous Pb–Ti–O precursor can be considered as two stages. The first stage (up to 10 h of milling) is mainly a mechanical process, in which the mechanical activation greatly refines the coprecipitated precursor. The second stage (longer than 10 h) includes both mechanical and chemical processes. At the initiation of the second stage, the precursor continues to be refined slightly. When the particle size becomes small enough, the components in the sample in the Pb–Ti–O system become unstable and reactive. The energy provided by mechanical activation is enough to trigger the formation of PT nuclei that normally occurs upon postcalcination. Longer milling time produces higher density of PT nuclei. The results from the postannealing (to be discussed in the next section) support this suggestion.

B. Growth mechanism and activation energies

In order to study the mechanical activation effects on the crystallization of the PT phase, both the precursor and me-

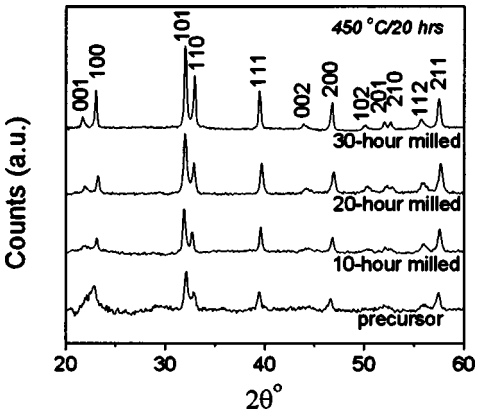

FIG. 4. XRD patterns of calcined samples at 450 °C for 20 h.

chanically activated samples were calcined at 425, 450, and 475 °C for 10, 13, 16, and 20 h at each temperature. Figure 4 shows the XRD patterns of the 450 °C/20 h calcined samples, which clearly indicates that the predominant tetragonal PT phase can be formed in all four starting materials. By integrating the area under the (111) peak and normalizing to the same peak of the respective fully transformed PT samples (650 °C/30 h), the amount of the crystallized tetragonal PT phase in all samples was measured.[16,17] As shown in Fig. 5, it can be clearly observed that the fraction of the crystallized PT phase is much higher for the 20- and 30-h-milled samples. Considering of the significant difference among the starting materials, it is reasonable to attribute this higher fraction of PT phase in the longer milled samples to the existence of PT crystallites. These PT crystallites act as seeds for PT phase growth during calcination.

If the crystallization of tetragonal PT phase can be considered as a nucleation and growth process, then by plotting the fraction of crystallized PT phase as a function of calcination time, the result should show a good agreement with the Avrami model,[18] where the relationship between volume fraction x and calcination time t is given by

$$x = 1 - \exp(-kt^n) \tag{1}$$

where n is a constant dependent on the nucleation and growth mechanism, and k is the rate constant. Under isothermal conditions, the experimental data can be better fitted according to the following linear transformation of the above equation:

$$\ln[-\ln(1-x)] = \ln k + n \ln t. \tag{2}$$

Figure 6 shows the plots of $\ln[-\ln(1-x)]$ as a function of $\ln t$. The rate constants were determined from the intercept with ordinate axe at each isothermal temperature. As shown in Table I, the rate constants for samples with longer milling time (which have a higher density of PT nuclei) were much larger than that of the precursor or samples with shorter milling time. In this work, the temperature dependence of k showed an apparent Arrhenius relationship:[19]

$$k = A \exp(-E_a/RT), \tag{3}$$

where A is the preexponential (frequency) factor, E_a the apparent activation energy of crystallization, and R the molar gas constant. The straight lines in the $\ln k$ vs $1000/T$ plots (Fig. 7) with very good correlation coefficients were clearly seen. The activation energy E_a, shown in Table I, was then determined from the slope of the plot. The activation energies calculated were 249 ± 6 kJ/mol for the precursor, 217 ± 5, 153 ± 3, and 97 ± 7 kJ/mol for 10-, 20-, and 30-h-milled samples, respectively. It is clear that the activation energy was dramatically lowered by the mechanical activations for more than 10 h. The above results suggest that an increase in the density of the PT nuclei which were derived from the mechanical activation and acted as PT seeds during the postcalcination can dramatically enhance the crystallization kinetics and lower the activation energy.

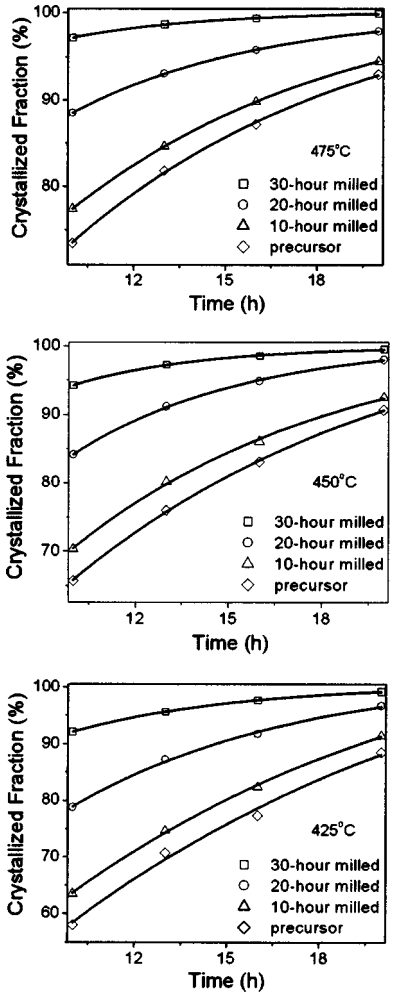

FIG. 5. Isothermal kinetics for the $PbTiO_3$ crystallization at 425, 450, and 475 °C as a function of the calcination duration.

C. Effect of particle size on the structure and unit cell volume

Figure 8 shows the XRD patterns of the 30-h-milled samples calcined up to 600 °C for a fixed period of 1 h. The XRD pattern of the precalcined sample shows one near-symmetric diffraction peak at 32.1° characterizing the pseudocubic structure,[9] and this peak becomes asymmetric after a relative low temperature (350 °C) calcination. Upon calcination at 450 °C, this peak sharpens and a shoulder peak

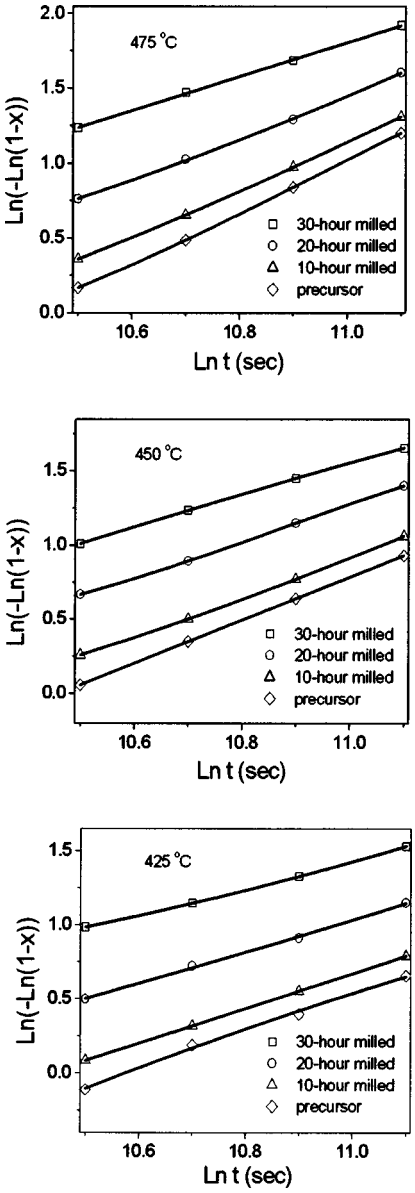

FIG. 6. Avrami plots for the $PbTiO_3$ crystallization at 425, 450, and 475 °C as a function of the ball milling time.

belonging to the (110) diffraction appears as a result, while the intensity of all peaks increases considerably. At this temperature, the PT phase experiences a rapid growth. After annealing at higher temperatures, the XRD peaks sharpen continuously reflecting the bigger size and better crystallinity of the PT nanocrystal particles. In the XRD pattern of the

TABLE I. Kinetic constant, k, and activation energy, E_a, for the crystallization of precursor, 10, 20, and 30-h-milled samples.

	k (s^{-1})			
Temperature (K)	Precursor	10-h milled	20-h milled	30-h milled
698	1.23×10^{-4}	1.65×10^{-4}	5.00×10^{-4}	3.62×10^{-3}
723	5.53×10^{-4}	6.62×10^{-4}	1.29×10^{-3}	7.37×10^{-3}
748	1.84×10^{-3}	2.03×10^{-3}	2.74×10^{-3}	1.29×10^{-2}
E_a (kJ/mol)	249±6	217±5	153±3	97±7

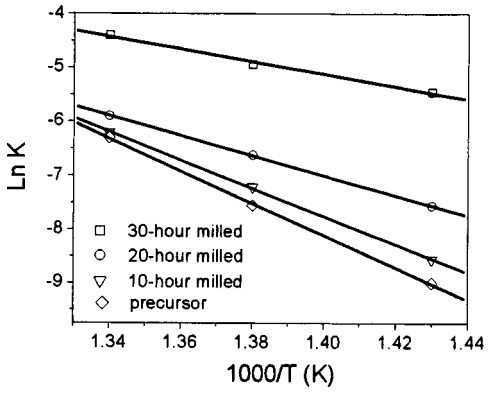

FIG. 7. Arrhenius plots of crystallization rate constant for calcined samples.

600 °C-annealed sample, the peak at 32.1° splits completely into two peaks at 31.5° and 32.4°, corresponding to the (101) and (110) planes of the PT phase with a tetragonal structure.[13] Note that this splitting from one symmetric peak to two peaks occurs gradually indicating that the structure of the PT crystal transforms from pseudocubic to tetragonal within the postcalcination process,[9] which is attributed to the size-effect of the nanoparticles. A nanocrystalline material shows a pseudocubic structure when the particles are very small.[20,21] With the increase in particle size, the material gradually assumes its bulk structure, the tetragonal phase in this case.

In order to study the size effect of nanoparticles on the structure of the PT phase, detailed analysis of the XRD results shown in Fig. 8 was carried out. Figure 9 plots the dependence of the tetragonal distortion (c/a) and the unit cell volume of the PT phase on the particle size. In this work, the average particle size was calculated from the full width at half-maximum (FWHM) of the (111) diffraction peak using the Scherrer equation which assumes the small crystallite size to be the only case of line broadening:[22]

$$D = K\lambda/B\cos\theta, \tag{4}$$

where D is the particle diameter, λ is the x-ray wavelength, B is the FWHM of the diffraction line, θ is the angle of diffraction, and the constant $K \approx 1$. The tetragonal distortion (c/a) and volume of unit cell were derived by calculating

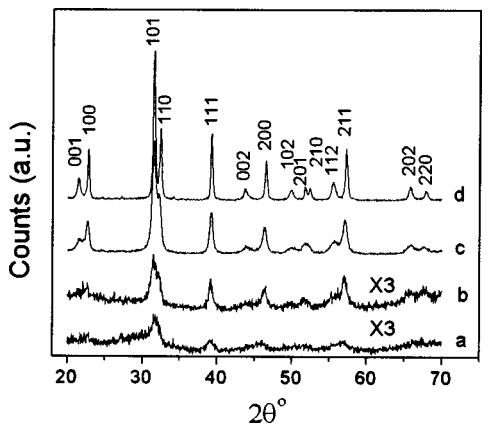

FIG. 8. XRD patterns of (a) 30-h-mechanically activated precursor and that calcined at (b) 350 °C, (c) 450 °C, and (d) 600 °C for 1 h.

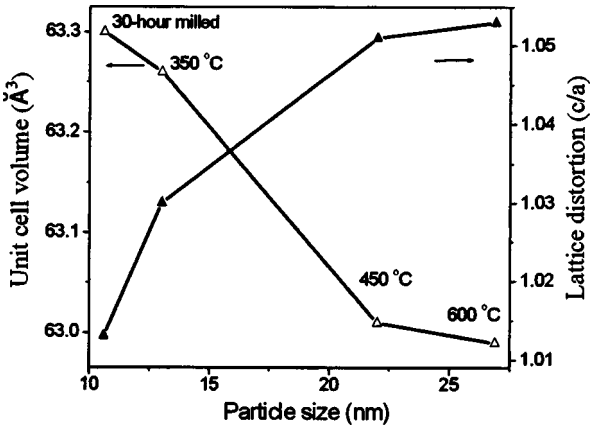

FIG. 9. c/a ratio and cell volume of the 30-h-mechanically activated precursor before and after postcalcination as the function of the particle size.

the fitting results of the two strongest peaks (101) and (110) using Gauss functions. From Fig. 9, it is obvious that the tetragonal distortion (c/a) shows a monotonic increase with the growth of PT phase, while the volume of the unit cell decreases with the increase of particle size. This increase in the tetragonal distortion (c/a) which indicates the structure transformation from pseudocubic to tetragonal has been attributed to the size effect of the PT particles in nanometer scale.[20,21] Interestingly, the unit cell volume decreases dramatically after calcination at 450 °C when the particle size shows an apparent increase. For larger particle sizes obtained at higher temperature the PT unit cell volume is almost constant. In addition, it is noted that this dramatic reduction of unit cell volume occurs when the diffraction peaks are sharpened and strengthened.

Raman scattering was also used to study the size effect during the postcalcination process and the Raman results support the conclusions drawn from the XRD analysis. Figure 10 shows the Raman spectra of the same samples as in the XRD analysis (Fig. 8). The pseudocubic structure of PT crystal formed in the 30-h-mechanically activated sample was clearly reflected in its Raman spectrum. As shown in Fig. 10(a), only one relatively sharp peak at ~300 cm^{-1} and

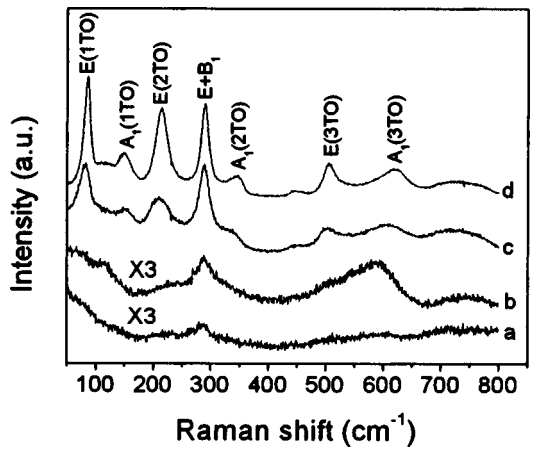

FIG. 10. Raman spectra of (a) 30-h-mechanically activated precursor and that calcined at (b) 350 °C, (c) 450 °C, and (d) 600 °C for 1 h.

a strong background in the low frequency region (below 100 cm^{-1}) were clearly observed. These are significant characteristics of the PT crystal with a high symmetrical structure as reported in the Raman study of PT structure phase transition.[15] After calcination, the well-known Raman modes belonging to tetragonal PT phase appear, indicating the establishment of the tetragonal phase. With increase in calcination temperature, the $E(1TO)$ and $E(2TO)$ modes show a blueshift while the position of the $E+B_1$ mode remains constant, all of which can be attributed to the size effect of the PT nanoparticles.[21,23,24]

IV. CONCLUSIONS

The effects of mechanical activation on the formation of $PbTiO_3$ powder from amorphous Pb–Ti–O precursor synthesized by the chemical coprecipitation method have been studied. The mechanical activation can be characterized by two stages: the size reduction of the starting materials for shorter milling time, and formation of the PT crystallites for longer milling duration. Acting as seed particles, these PT crystallites can dramatically lower the activation energy and enhance the crystallization kinetics during the postcalcination processes. Consequently, the onset crystallization temperature was also lowered. The PT phase with particles smaller than 15 nm is pseudocubic while that with larger size has the typical tetragonal structure. The size effect may be the dominant factor in determining the unit cell volume.

[1] C. Chardler, C. Roger, and M. Hampden-Smith, Chem. Rev. **93**, 1205 (1993).
[2] W. C. Hendricks, S. B. Desu, and C. H. Peng, Chem. Mater. **6**, 1955 (1994).
[3] J. S. Wright and L. F. Francis, J. Mater. Res. **8**, 1712 (1993).
[4] J. Fang, J. Wang, S. C. Ng, C. H. Chew, and L. M. Gan, J. Mater. Sci. **34**, 1943 (1999).
[5] M. H. Lee and B. C. Choi, J. Am. Ceram. Soc. **74**, 2309 (1991).
[6] Y. Ohara, K. Koumoto, T. Shimizu, and H. Yanagida, J. Mater. Sci. **30**, 263 (1995).
[7] L. B. Kong, W. Zhu, and O. K. Tan, Ferroelectrics **230**, 281 (1999).
[8] J. M. Xue, D. M. Wan, S. E. Lee, and J. Wang, J. Am. Ceram. Soc. **82**, 1641 (1999).
[9] E. R. Leite, E. C. Paris, and E. Longo, J. Am. Ceram. Soc. **83**, 1539 (2000).
[10] J. Wang, D. M. Wan, J. M. Xue, and W. B. Ng, J. Am. Ceram. Soc. **82**, 477 (1999).
[11] J. M. Xue, D. M. Wan, S. E. Lee, and J. Wang, J. Am. Ceram. Soc. **82**, 1687 (1999).
[12] J. Wang, J. M. Xue, D. M. Wan, and B. K. Gan, J. Solid State Chem. **154**, 321 (2000).
[13] JCPDS-International Centre for Diffracton Data 06-0452.
[14] T. Yu, Z. X. Shen, J. M. Xue, and J. Wang, Mater. Chem. Phys. **75**, 216 (2002).
[15] P. S. Dobal, S. Bhaskar, S. B. Majumder, and R. S. Katiyar, J. Appl. Phys. **86**, 828 (1999).
[16] J. Tartaj, J. F. Fernandez, C. Moure, and P. Daran, J. Eur. Ceram. Soc. **18**, 229 (1998).
[17] Z. Huang, Q. Zhang, and R. W. Whatmore, J. Appl. Phys. **85**, 7355 (1999).
[18] M. Avrami, J. Chem. Phys. **7**, 1103 (1939); **9**, 177 (1941).
[19] S. Ranganathan and M. V. Heimendahl, J. Mater. Sci. **16**, 2401 (1981).
[20] S. Chattopadhyay, P. Ayyub, V. R. Palkar, and M. Multani, Phys. Rev. B **52**, 13177 (1995).
[21] K. Ishikawa, K. Yoshikawa, and N. Okada, Phys. Rev. B **37**, 5852 (1988).
[22] A. J. C. Wilson, Proc. Phys. Soc. London **80**, 286 (1962).
[23] W. L. Zhang, B. Jiang, P. L. Zhang, J. M. Ma, H. M. Cheng, Z. H. Yang, and L. X. Li, J. Phys.: Condens. Matter **5**, 2619 (1993).
[24] K. Ishikawa, T. Nomura, N. Okada, and K. Takada, Jpn. J. Appl. Phys., Part 1 **35**, 5196 (1996).